Coupled Systems Mechanics, *Vol. 14, No. 6 (2025) 531-549*
https://doi.org/10.12989/csm.2025.14.6.531

Study and analysis of the mechanical response of Carbon/Glass hybrid composite plates

Belkacem Adim*[1,2], Tahar Hassaine Daouadji[2,3] and Ayed Eid Alluqmani[4]

[1]*Department of Civil, Mechanical and Transportation Engineering, Tissemsilt University, Tissemsilt, Algeria*
[2]*Geomatics and Sustainable Development Laboratory, Ibn Khaldoun University, Tiaret, Algeria*
[3]*Department of Civil Engineering, Ibn Khaldoun University, Tiaret, Algeria*
[4]*Department of Civil Engineering, Faculty of Engineering, Islamic University of Madinah, Al-Madinah Al-Munawara, Prince Naif Ibn Abdulaziz, Al Jamiah, Medina 42351, Saudi Arabia*

(Received March 4, 2025, Revised November 22, 2025, Accepted December 8, 2025)

Abstract. In the present manuscript, we focus our investigation on the intralaminar hybrid composite plates, where the bending behavior is addressed employing a reliable and efficient refined high-order theory. The present refined theory successfully simulates the plate's real behavior by considering the shear effect in deformations, counting only four variables in the mathematical formulation and ensuring the parabolic distribution of these shear strains and stresses. Also, the nullity of shear stresses at the plate's top and bottom faces is guaranteed by the present refined theory. Unlike conventional composites, hybrid composite materials offer compelling features like the opportunity to create new and advantageous structures by varying the fiber combinations and proportions. This variation leads to diverse kinds of hybrid composites, each of which is intended for specific applications, depending on the characteristics expected by manufacturers. The present theory's numerical and graphical results are validated against other literature-issued high-order theories. This validation is followed by a parametric study to highlight the effect of various parameters on the behavior of hybrid composites. Based on this research, we can conclude that the suggested refined theory is reliable, precise and efficient for investigating the bending behavior of intralaminar hybrid composite plates.

Keywords: bending behavior; intralaminar hybrid composites; laminated plate; refined higher-order theory; shear stress

1. Introduction

Over the years, composite materials have become crucial for engineering applications, thanks to their exceptional characteristics that enhance the structures performance in different fields including mechanical, civil and aerospace engineering. Their features like stiffness, lightweight, and resistance to environmental conditions make them the perfect fit for industrial applications varying from structural elements in constructions to diverse components in vehicles and airplanes manufacturing (Keller 2024, Georgantzinos *et al.* 2023, Drobnjak 2023). For example, fiber

*Corresponding author, Professor, E-mail: adim.belkacem@univ-tissemsilt.dz

 ISSN: 2234-2184 (Print), 2234-2192 (Online)

reinforced polymer composites (FRP) are more and more employed for retrofitting and strengthening reinforced concrete structures, emphasizing their usefulness and efficiency in civil engineering field (Drobnjak 2023). Furthermore, developments in composite characterization techniques and manufacturing process, like additive manufacturing and nanotechnology for instance, are fostering development and improving processes of design, which is crucial for boosting their efficiency. The increasing need for composites, emphasizes their importance in producing efficient and sustainable innovative solutions (Georgantzinos *et al.* 2023, Kulkarni and Boppana 2023).

The progress of plates higher-order theories has helped greatly in the study of various advanced structures for countless materials, mainly composite plates. Primarily, classical laminated plates theories like Love-Kirchhoff (CPT) Theory and the first order high deformation theory (FSDT) representing the base foundation of plates theories, nevertheless they underestimated or neglected entirely the impact shear strains and stresses). The Higher-Order Shear Deformation Theories (HSDTs) came to remedy these shortcomings by introducing nonlinear variations of shear strains, improving precision for all kinds of plates (thick and thin plates) (De Matos and Júnior 2024, Thai and Kim 2013, Henni *et al.* 2021). Recent advancements including theories using couple stress and micropolar models, which employ Fourier series expansions to describe strain and stress distributions more precisely throughout the plate's thickness (Zozulya 2018a, b). These developments made it easier to investigate the behavior of various materials, like orthotropic laminated plates for instance, leading to a better understanding of material characteristics (Furtmüller and Adam 2022).

The investigation of bending behavior of composite plates is indispensable for numerous engineering applications, especially in automotive and aerospace domains, where used materials required to show high qualities, to be light, and have a good mechanical resistance. Studies pointed out that composite materials widely improve mechanical behavior against applied loads (Kirad *et al.* 2023, Sundeep and Baddepudi 2023). Advanced analytical methods like Higher Order Shear Deformation Theory (HSDT) stated in the previous section are used to precisely calculate stress and strains distributions in composite laminates (Nadaf and Fernandes 2023). These theories take into account the complexities of materials behavior, ranging from stress variations across the plate's thickness to the impact of fiber's orientation (Latheswary *et al.* 2003, Daouadji *et al.* 2016a, Adim and Daouadji 2024). Researches revealed that employing HSDT enhance calculations precision which is crucial for guaranteeing the plates structural integrity in real-world applications (Nadaf and Fernandes 2023).

Hybrid composites emerged as a major leap forward in materials science, joining several component materials to improve physical, mechanical, and thermal characteristics. These hybrid composites can be manufactured using numerous techniques to ensure perfect quality and eliminated or at least limiting fabrication defects (Jain and Kathuria 2024). Recent researches have investigated the integration of agricultural waste fibers, like Borassus and Crotalaria, as reinforcements, exhibiting considerable enhancements in water absorption resistance and tensile strength, therefore encouraging sustainability (Ramu *et al.* 2024). In the aerospace field, hybrid nanocomposites introduce metallic matrix with nano-reinforcements like graphene and carbon nanotubes, show extraordinary stiffness-to-weight ratios and resilience (Monteiro and Simões 2024). The continuing investigations stresses on optimizing manufacturing techniques to avoid nanoparticle agglomeration and improve material characteristics, laying the foundations for groundbreaking applications in numerous fields, including energy storage and nanomedicine (Alarifi and Asmatulu 2023).

Furthermore, some research, such as those described in (Sahu *et al.* 2022a, Dewangan and Panda 2021, Kumar *et al.* 2023, Pandey *et al.* 2020, Sahu *et al.* 2022b), use both computational and experimental methods to investigate the mechanical behavior of composite materials, particularly hybrid fiber-reinforced composites. In order to predict the deflection, vibration, and dynamic responses of composite panels under a variety of loading conditions, such as thermal environments and structural damage, these studies use higher-order finite element methods. Experimental validation shows a strong agreement with these theoretical models (Rabahi *et al.* 2014, Daouadji *et al.* 2016c).

The literature review shows a notable shortage in research that concurrently inspects several aspects of the bending behavior of hybrid composite laminates, particularly for intralaminar hybrid arrangements featuring several fiber types in the same layer. While such hybridization presents intricate mechanical interactions, only few studies methodically examine how particular fiber combinations effect bending stiffness, deformation and stress distributions. This gap is further strengthened by the lack of investigations employing refined high-order shear deformation theories, which offer improved precision for modeling through-thickness effects without excessive computational cost. Collectively, these deficits emphasize the need for more inclusive investigations that include intralaminar hybridization strategies, and innovative yet effective theoretical studies to better describe and predict the bending behavior of laminated hybrid composite plates.

This study employs a new refined high-order shear deformation theory that efficiently represents complex through-thickness stress and strains in hybrid composite laminates while sustaining mathematical simplicity and computing efficiency. In contrast to classical or first-order theories, the present refined theory incorporates higher-order displacement fields that remove the requirement for shear correction factors and more accurately represent transverse shear strains and stresses. Furthermore, the present refined theory avoids the mathematical complexity of the third-order or layer-wise approaches, presenting a balanced and manageable formulation.

The main purpose of the present manuscript is to investigate how fiber combinations in intralaminar hybrid composites impact the mechanical behavior of composite laminates via a reliable and accurate refined high-order shear deformation theory. Furthermore, this study's objective is to improve hybrid composites handling for modern applications by recommending a simpler mathematical model to predict the optimal plate's configuration, like geometry, fiber combination, stacking sequence, and fibers orientation, to respond to various criteria imposed by industries, for instance: mechanical conditions and economy.

2. Hybrid composite material properties

The vast majority of composite structures are composed of a single type of fiber and a matrix; therefore, the composite's characteristics are dependent on this specific single fiber. Therefore, the whole structure is susceptible to failure or damage if this fiber has a weakness, such as poor stiffness or fragility.

Hybrid composite plates include a combination of numerous types of fibers, usually two. This promising advancement offers a number of benefits, such as reduced production costs or enhanced properties of one of the fibers, such as electrical conductivity, strength, resilience, durability at high temperatures, and longevity.

The longitudinal Young's modulus of the hybrid composite plate considered in the present

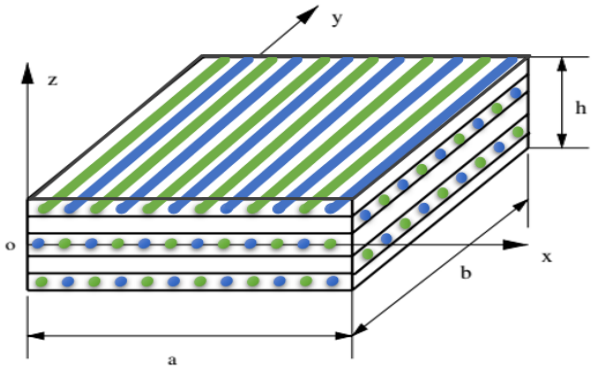

Fig. 1 Fiber arrangement and coordinate system for an intralayer hybrid plate

investigation is expressed as follow (Vaseliev and Morozov 2001)

$$E_1 = E_{f1}V_{f1} + E_{f2}V_{f2} + E_mV_m \tag{1}$$

Where E_1 is hybrid composite's longitudinal Young's modulus. E_{f1}, E_{f2} are the Young's moduli of the first and the second type of fibers respectively and E_m is the matrix Young's modulus. V_{f1}, V_{f2} are the volume fraction of the first and the second type of fibers respectively and V_m is the matrix volume fraction, given by

$$V_{f1} + V_{f2} + V_m = 100\% \text{ and } V_{f1} + V_{f2} = V_f \tag{2}$$

Assuming that

$$w_f = \frac{V_{f1}}{V_f} \tag{3}$$

With w_f is the percentage (ratio) of the first type of fiber over the fiber's total volume fraction. By combining Eq. (1) with Eq. (3) we get

$$E_1 = V_f[E_{f1}w_f + E_{f2}(1 - w_f)] + E_mV_m \tag{4}$$

By analogy, the Poisson's ratio can be determined as

$$\nu_{12} = V_f[\nu_{f1}w_f + \nu_{f2}(1 - w_f)] + \nu_mV_m \tag{5}$$

The shear modulus of the fibers and the matrix are expressed according to Berthelot (2010) as follow

$$G_m = \frac{E_m}{2(1+\nu_m)} \tag{6}$$

$$G_{f1} = \frac{E_{f1}}{2(1+\nu_{f1})} \tag{7}$$

$$G_{f2} = \frac{E_{f2}}{2(1+\nu_{f2})} \tag{8}$$

Where G_{f1}, G_{f2} are the shear modulus of the first and the second type of fibers respectively and

G_m is the matrix shear modulus, Moreover the shear modulus of total fibers is illustrated by

$$G_f = G_{f1}w_f + G_{f2}(1 - w_f) \tag{9}$$

The matrix and fibers compressibility moduli are given by

$$k_m = \frac{E_m}{3(1-2\nu_m)} \tag{10}$$

$$k_f = \frac{E_{f1}w_f}{3(1-2\nu_{f1})} + \frac{E_{f2}(1-w_f)}{3(1-2\nu_{f2})} \tag{11}$$

The matrix and fibers lateral compressibility moduli are given by

$$K_m = k_m + \frac{G_m}{3}, K_f = k_f + \frac{G_f}{3} \tag{12}$$

The plate's shear moduli are as follow

$$G_{12} = G_m \frac{G_f(1+V_f)+G_m(1-V_f)}{G_f(1-V_f)+G_m(1+V_f)}, G_{13} = G_{12} \tag{13}$$

$$G_{23} = G_m\left(1 + \frac{V_f}{\frac{G_m}{G_f-G_m}+V_m\frac{k_m+7G_m/3}{2k_m+8G_m/3}}\right) \tag{14}$$

The plate's lateral compressibility modulus is given by

$$K_L = K_m + \frac{V_f}{\frac{1}{k_f-k_m+(G_f-G_m)/3}+\frac{1-V_f}{k_m+(4/3)G_m}} \tag{15}$$

Based on Eqs. (4)-(15), the plate's transversal Young's modulus is expressed as

$$E_2 = \frac{2}{\frac{1}{2K_L}+\frac{1}{2G_{23}}+\frac{2(\nu_{12})^2}{E_1}} \tag{16}$$

3. Mathematical formulation

3.1 Displacements, strains and stresses

Based on the assumptions of the refined high order shear deformation theory, the displacement field for the present study can be expressed by

$$\begin{gathered} u(x,y,z) = u_0(x,y) - z\frac{\partial w_b}{\partial x} - f(z)\frac{\partial w_s}{\partial x} \\ v(x,y,z) = v_0(x,y) - z\frac{\partial w_b}{\partial y} - f(z)\frac{\partial w_s}{\partial y} \\ w(x,y,z) = w_b(x,y) + w_s(x,y) \end{gathered} \tag{17}$$

Where *f*(*z*) represents shape functions that determine the distribution of the transverse shear strains and stresses through the plate's thickness, u_0 and v_0 are the plate's mid-plane displacements in the *x* and *y* directions, respectively. For the transverse displacement, w_b and w_s are the bending and shear components, respectively. This feature guarantees that the plate's upper and lower faces exhibit zero transverse shear stress. The present refined function of the displacement field

employed in the analysis to ensure the parabolic distributions of transverse shear stresses over the thickness of the plate and is given according to Xiang and Kang (2013) by

$$f(z) = \frac{16z^5}{5h^4} \tag{18}$$

The strains can be obtained from the displacement field in Eq. (17), these stains can be given by

$$\varepsilon_x = \frac{\partial u_0}{\partial x} - z\frac{\partial^2 w_b}{\partial x^2} - f(z)\frac{\partial^2 w_s}{\partial x^2},\ \varepsilon_y = \frac{\partial v_0}{\partial y} - z\frac{\partial^2 w_b}{\partial y^2} - f(z)\frac{\partial^2 w_s}{\partial y^2},\ \varepsilon_z = 0 \tag{19a}$$

$$\gamma_{xy} = \frac{\partial u_0}{\partial y} + \frac{\partial v_0}{\partial x} - 2z\frac{\partial^2 w_b}{\partial x \partial y} - 2f(z)\frac{\partial^2 w_s}{\partial x \partial y},\ \gamma_{yz} = g(z)\frac{\partial w_s}{\partial y},\ \gamma_{xz} = g(z)\ \frac{\partial w_s}{\partial x} \tag{19b}$$

Assuming that

$$\varepsilon_x^0 = \frac{\partial u_0}{\partial x},\ k_x^b = -\frac{\partial^2 w_b}{\partial x^2},\ k_x^s = -\frac{\partial^2 w_s}{\partial x^2},\ \varepsilon_y^0 = \frac{\partial v_0}{\partial y},\ k_y^b = -\frac{\partial^2 w_b}{\partial y^2},\ k_y^s = -\frac{\partial^2 w_s}{\partial y^2},\ \gamma_{xy}^0 = \frac{\partial u_0}{\partial y} + \frac{\partial v_0}{\partial x} \tag{20a}$$

$$k_{xy}^b = -2\frac{\partial^2 w_b}{\partial x \partial y},\ k_{xy}^s = -2\frac{\partial^2 w_s}{\partial x \partial y},\ \gamma_{yz}^s = \frac{\partial w_s}{\partial y},\ \gamma_{xz}^s = \frac{\partial w_s}{\partial x} \text{ and } g(z) = 1 - \frac{df(z)}{dz} \tag{20b}$$

The strains can be expressed as follow

$$\varepsilon_x = \varepsilon_x^0 + z\,k_x^b + f(z)k_x^s, \varepsilon_y = \varepsilon_y^0 + z\,k_y^b + f(z)k_y^s, \varepsilon_z = 0 \tag{21a}$$

$$\gamma_{xy} = \gamma_{xy}^0 + z\,k_{xy}^b + f(z)\,k_{xy}^s,\quad \gamma_{yz} = g(z)\,\gamma_{yz}^s,\ \gamma_{xz} = g(z)\,\gamma_{xz}^s \tag{21b}$$

The stress relations of hybrid composite plates can be deduced by applying the Hooke's law, and can be given by

$$\begin{Bmatrix}\sigma_x\\ \sigma_y\\ \tau_{xy}\end{Bmatrix} = \begin{bmatrix}\bar{Q}_{11} & \bar{Q}_{12} & \bar{Q}_{16}\\ \bar{Q}_{12} & \bar{Q}_{22} & \bar{Q}_{26}\\ \bar{Q}_{16} & \bar{Q}_{26} & \bar{Q}_{66}\end{bmatrix}\begin{Bmatrix}\varepsilon_x\\ \varepsilon_y\\ \gamma_{xy}\end{Bmatrix} \tag{22a}$$

$$\begin{Bmatrix}\tau_{yz}\\ \tau_{xz}\end{Bmatrix} = \begin{bmatrix}\bar{Q}_{44} & \bar{Q}_{45}\\ \bar{Q}_{45} & \bar{Q}_{55}\end{bmatrix}\begin{Bmatrix}\gamma_{yz}\\ \gamma_{xz}\end{Bmatrix} \tag{22b}$$

With $(\varepsilon_x, \varepsilon_y, \gamma_{xy}, \gamma_{yz}, \gamma_{xz})$ and $(\sigma_x, \sigma_y, \tau_{xy}, \tau_{yz}, \tau_{xz})$ are the normal and shear strains and stresses components, respectively.

The stiffness coefficients $\bar{Q}_{ij}$, can be given according to Adim *et al.* (2016) by

$$\begin{aligned}
\bar{Q}_{11} &= Q_{11}\cos^4\theta + Q_{22}\sin^4\theta + 2(Q_{12} + 2Q_{66})\sin^2\theta\cos^2\theta\\
\bar{Q}_{12} &= (Q_{11} + Q_{22} - 4Q_{66})\sin^2\theta\cos^2\theta + Q_{12}(\cos^4\theta + \sin^4\theta)\\
\bar{Q}_{16} &= (Q_{11} - Q_{12} - 2Q_{66})\sin\theta\cos^3\theta + (Q_{12} - Q_{22} + 2Q_{66})\sin^3\theta\cos\theta\\
\bar{Q}_{22} &= Q_{11}\sin^4\theta + 2(Q_{12} + 2Q_{66})\sin^2\theta\cos^2\theta + Q_{22}\cos^4\theta\\
\bar{Q}_{26} &= (Q_{11} - Q_{12} - 2Q_{66})\cos\theta\sin^3\theta + (Q_{12} - Q_{12} - 2Q_{66})\sin\theta\cos^3\theta\\
\bar{Q}_{66} &= [(Q_{11} + Q_{22} - 2(Q_{12} + Q_{66})]\cos^2\theta\sin^2\theta + Q_{66}(\sin^4\theta + \cos^4\theta)\\
\bar{Q}_{44} &= Q_{44}\cos^2\theta + Q_{55}\sin^2\theta\\
\bar{Q}_{45} &= (Q_{55} - Q_{44})\cos\theta\sin\theta\\
\bar{Q}_{55} &= Q_{55}\cos^2\theta + Q_{44}\sin^2\theta
\end{aligned} \tag{23}$$

3.2 Equilibrium equations

Using the principle of virtual displacements, we derive the equilibrium equations of the hybrid composite plate

$$U - V = 0 \tag{24}$$

Where U is the deformation energy and V is the work of external loads. Using the principle of virtual works to obtain equilibrium equation leads to the following integration

$$\int_V (\sigma_x \delta\varepsilon_x + \sigma_y \delta\varepsilon_y + \tau_{xy}\delta\gamma_{xy} + \tau_{yz}\delta\gamma_{yz} + \tau_{xz}\delta\gamma_{xz})dV - \int_A q\delta(w_b + w_s)dA = 0 \tag{25}$$

Where $\boldsymbol{A}$ is the upper section of the plate and $\boldsymbol{q}$ is the applied load.

Following the mathematical development detailed by Daouadji *et al.* (2016b), the equations of equilibrium are expressed by

$$\begin{gathered}
\delta u_0 : N_{x,x} + N_{xy,y} = 0 \\
\delta v_0 : N_{xy,x} + N_{y,y} = 0 \\
\delta w_b : M^b_{x,xx} + 2M^b_{xy,xy} + M^b_{y,yy} + q = 0 \\
\delta w_s : M^s_{x,xx} + 2M^s_{xy,xy} + M^s_{y,yy} + S^s_{xz,x} + S^s_{yz,y} + q = 0
\end{gathered} \tag{26}$$

Knowing that, N, M and S^s are the resultants of stresses

3.3 Navier's analytical solutions for hybrid composite plates

The Navier analytical solutions can be developed for hybrid laminates with two sets of simply supported boundary conditions.

3.3.1 For hybrid cross-ply laminates

For cross-ply hybrid laminates the boundary conditions set by Navier are fulfilled by the following expressions

$$\begin{gathered}
u_0 = \sum_{m=1}^{\infty}\sum_{n=1}^{\infty} U_{mn}\, cos(\lambda x)\, sin(\mu\ y) \\
v_0 = \sum_{m=1}^{\infty}\sum_{n=1}^{\infty} V_{mn}\, sin(\lambda x)\, cos(\mu\ y) \\
w_b = \sum_{m=1}^{\infty}\sum_{n=1}^{\infty} W_{bmn}\, sin(\lambda x)\, sin(\mu\ y) \\
w_s = \sum_{m=1}^{\infty}\sum_{n=1}^{\infty} W_{smn}\, sin(\lambda x)\, sin(\mu y)
\end{gathered} \tag{27}$$

Where U_{mn},V_{mn}, W_{bmn} and W_{smn} unknown variables needs to be determined, and $\lambda = \frac{m\pi}{a}$ and $\mu = \frac{n\pi}{b}$.

The applied transverse load $\boldsymbol{q}$ is also expressed in the double-Fourier sinus series by

$$q(x,y) = \sum_{m=1}^{\infty}\sum_{n=1}^{\infty} Q_{mn}\, sin(\lambda x)\, sin(\mu y) \tag{28}$$

Replacing Eqs. (27) and (28) into Eq. (26), the Navier analytical solution for cross-ply hybrid laminates can be deduced from equations

$$\begin{bmatrix} a_{11} & a_{12} & a_{13} & a_{14} \\ a_{12} & a_{22} & a_{23} & a_{24} \\ a_{13} & a_{23} & a_{33} & a_{34} \\ a_{14} & a_{24} & a_{34} & a_{44} \end{bmatrix} \begin{Bmatrix} U_{mn} \\ V_{mn} \\ W_{bmn} \\ W_{smn} \end{Bmatrix} = \begin{Bmatrix} 0 \\ 0 \\ q \\ q \end{Bmatrix} \tag{29}$$

With

$$\begin{gathered} a_{11} = A_{11}\lambda^2 + A_{66}\mu^2,\ a_{12} = \lambda\mu(A_{12} + A_{66}),\ a_{13} = -B_{11}\lambda^3,\ a_{14} = -B^s_{11}\lambda^3 \\ a_{22} = A_{66}\lambda^2 + A_{22}\mu^2,\ a_{23} = B_{11}\mu^3,\ a_{24} = B^s_{11}\mu^3 \\ a_{33} = D_{11}\lambda^4 + 2(D_{12} + 2D_{66})\lambda^2\mu^2 + D_{22}\mu^4 \\ a_{34} = D^s_{11}\lambda^4 + 2(D^s_{12} + 2D^s_{66})\lambda^2\,\mu^2 + D^s_{22}\,\mu^4 \\ a_{44} = H^s_{11}\lambda^4 + 2(H^s_{12} + 2H^s_{66})\lambda^2\mu^2 + H^s_{22}\mu^4 + A^s_{55}\lambda^2 + A^s_{44}\mu^2 \end{gathered} \tag{30}$$

3.3.2 For hybrid angle-ply laminates

For angle-ply hybrid laminates the boundary conditions set by Navier are fulfilled by the following expressions

$$\begin{gathered} u_0 = \sum_{m=1}^{\infty}\sum_{n=1}^{\infty} U_{mn}\, sin(\lambda\, x)\, cos(\mu\, y) \\ v_0 = \sum_{m=1}^{\infty}\sum_{n=1}^{\infty} V_{mn}\, cos(\lambda\, x)\, sin(\mu y) \\ w_b = \sum_{m=1}^{\infty}\sum_{n=1}^{\infty} W_{bmn}\, sin(\lambda\, x)\, sin(\mu\, y) \\ w_s = \sum_{m=1}^{\infty}\sum_{n=1}^{\infty} W_{smn}\, sin(\lambda\, x)\, sin(\mu\, y) \end{gathered} \tag{31}$$

And Eq. (27) is exhibited in the following expression

$$\begin{gathered} a_{11} = A_{11}\lambda^2 + A_{66}\mu^2,\ a_{12} = \lambda\mu\,(A_{12} + A_{66}),\ a_{13} = -(3B_{16}\lambda^2\mu + B_{26}\mu^3) \\ a_{14} = -(3B^s_{16}\lambda^2\mu + B^s_{26}\mu^3),\ a_{23} = -(B_{16}\lambda^3 + 3B_{26}\lambda\mu^2),\ a_{24} = -(B^s_{16}\lambda^3 + 3B^s_{26}\lambda\mu^2) \\ a_{22} = A_{66}\lambda^2 + A_{22}\mu^2,\ a_{33} = D_{11}\lambda^4 + 2(D_{12} + 2D_{66})\lambda^2\mu^2 + D_{22}\mu^4 \\ a_{34} = D^s_{11}\lambda^4 + 2(D^s_{12} + 2D^s_{66})\lambda^2\,\mu^2 + D^s_{22}\,\mu^4 \\ a_{44} = H^s_{11}\lambda^4 + 2(H^s_{12} + 2H^s_{66})\lambda^2\mu^2 + H^s_{22}\mu^4 + A^s_{55}\lambda^2 + A^s_{44}\mu^2 \end{gathered} \tag{32}$$

In the purpose of calculating strains and stresses for the hybrid composite plate using the present refined theory all we need to do is resolve equations system in Eq. (29).

4. Results and discussion

This section of the current study is de dedicated to the validation of the present refined theory, where numerous examples are exhibited and discussed in form of tables and figures to prove the efficiency and precision of the present theory in predicting the static behavior cross-ply and angle-ply hybrid plates. For the validation purposes, the present refined theory results are compared against other literature issued high order theories, namely: Pagano (1970) or 3D, Pandya and Kant (1988), Kant and Swaminathan (2002).

The material properties adopted in this validation section are:

$$E_1 = 25E_2,\ G_{12} = G_{13} = 0.5E_2,\ \ G_{23} = 0.2E_2, \nu_{12} = 0.25$$

For the parametric investigation section, we consider a laminated hybrid plate composed of two fiber types: glass and carbon, the matrix is made from epoxy. The following material properties are expressed by Berthelot (2005) as follow:

Fiber 1 (Carbon) : $E_{f1} = 380\ GPa, \nu_{f1} = 0.33$

Fiber 2 (Glass): $E_{f2} = 86\ GPa, \nu_{f2} = 0.22$

Matrix : $E_m = 3.45\ GPa, \nu_f = 0.3$

The dimensionless parameters are employed her to obtain various results

Table 1 Matrix size in high order theories

Theory	Matrix size
Pandya and Kant (1988)	9×9
Kant and Swaminathan (2002)	12×12
Present	4×4

Table 2 Variation of dimensionless deflection and stresses in a square simply supported two-layer (0°/90°) composite plate under transverse load

a/h	Theory	$\bar{w}$	$\bar{\sigma}_x$	$\bar{\sigma}_y$	$\bar{\tau}_{xy}$
5	3D (Pagano 1970)	1.7287	-0.7723	0.8036	-0.0586
	Pandya and Kant (1988)	1.6800	-0.7510	0.7720	-0.0557
	Kant and Swaminathan (2002)	1.7037	-0.7662	0.7662	-0.0572
	Present	1.6996	-0.8126	0.8126	-0.0555
10	3D (Pagano 1970)	1.2318	-0.7317	0.7353	-0.0540
	Pandya and Kant (1988)	1.2192	-0.7269	0.7273	-0.0533
	Kant and Swaminathan (2002)	1.2274	-0.7286	0.7286	-0.0539
	Present	1.2233	-0.7401	0.7401	-0.0533
20	3D (Pagano 1970)	1.1060	-0.7200	0.7206	-0.0529
	Pandya and Kant (1988)	1.1025	-0.7189	0.7186	-0.0527
	Kant and Swaminathan (2002)	1.1078	-0.7185	0.7185	-0.0530
	Present	1.1035	-0.7218	0.7218	-0.0527
100	3D (Pagano 1970)	1.0742	-0.7219	0.7219	-0.0529
	Pandya and Kant (1988)	1.0651	-0.7161	0.7161	-0.0525
	Kant and Swaminathan (2002)	1.0695	-0.7152	0.7152	-0.0527
	Present	1.0652	-0.7160	0.7160	-0.0525

$$\bar{w} = \frac{100h^3E_2}{q_0a^4}w(\frac{a}{2},\frac{b}{2}),\ \bar{\sigma}_x = \frac{h^2}{q_0a^2}\sigma_x(\frac{a}{2},\frac{b}{2}),\ \bar{\sigma}_y = \frac{h^2}{q_0a^2}\sigma_y(\frac{a}{2},\frac{b}{2})$$
$$\bar{\tau}_{xy} = \frac{h^2}{q_0a^2}\tau_{xy}(0,0),\ \bar{\tau}_{xz} = \frac{h}{q_0a}\tau_{xz}(0,\frac{b}{2}),\ \bar{\tau}_{yz} = \frac{h}{q_0a}\tau_{xz}(\frac{a}{2},0) \quad (33)$$

Table 1 clearly demonstrates that the present refined high-order shear deformation theory employed in this study provides a simpler formulation and improved computing efficiency relative to alternative high-order theories. Notably, it requires only four variables, whereas alternative approaches typically involve nine or even twelve, resulting in reduced complexity and enhanced time performance.

Table 2 exhibits dimensionless deflection and stresses of a two-layer square simply supported cross-ply (0°/90°) composite plates subjected to transverse load. From the numerical results shown in this table, it is evident that the present refined theory gives results comparable to those issued from other high order theories, namely: 3D (Pagano 1970), Pandya and Kant (1988), Kant and Swaminathan (2002). Especially for values of side to thickness ratio equal or greater than ten. From this comparison we can conclude that the present theory can predict accurately the bending behavior of laminated composite plate in terms of deflection and stresses using a reduced number of variables compared to other high order theories issued from literature.

Table 3 Variation of dimensionless deflection $\bar{w}$ of two layers simply supported cross-ply (0/90) Carbon/glass-epoxy hybrid square laminates as a function of fibers' volume fraction V_f

Carbon's fibers percentage w_f (%)		V_f								
Carbon	Glass	0.3	0.35	0.4	0.45	0.5	0.55	0.6	0.65	0.7
0%	100%	2.2347	2.2051	2.1862	2.1767	2.1758	2.1834	2.1994	2.2241	2.2586
10%	90%	2.0997	2.0672	2.0468	2.0369	2.0368	2.0461	2.0647	2.0932	2.1325
20%	80%	1.9853	1.9505	1.9288	1.9186	1.9190	1.9295	1.9500	1.9811	2.0238
30%	70%	1.8857	1.8492	1.8267	1.8163	1.8171	1.8286	1.8506	1.8837	1.9291
40%	60%	1.7976	1.7598	1.7367	1.7263	1.7275	1.7397	1.7629	1.7977	1.8453
50%	50%	1.7187	1.6801	1.6566	1.6462	1.6477	1.6605	1.6846	1.7208	1.7702
60%	40%	1.6474	1.6082	1.5845	1.5742	1.5759	1.5892	1.6141	1.6513	1.7021
70%	30%	1.5826	1.5430	1.5192	1.5090	1.5110	1.5246	1.5501	1.5880	1.6400
80%	20%	1.5233	1.4835	1.4597	1.4496	1.4518	1.4657	1.4916	1.5301	1.5830
90%	10%	1.7415	1.6159	1.5289	1.4688	1.4290	1.4053	1.3953	1.3976	1.4117
100%	0%	1.6936	1.5663	1.4787	1.4185	1.3787	1.3552	1.3453	1.3478	1.3620

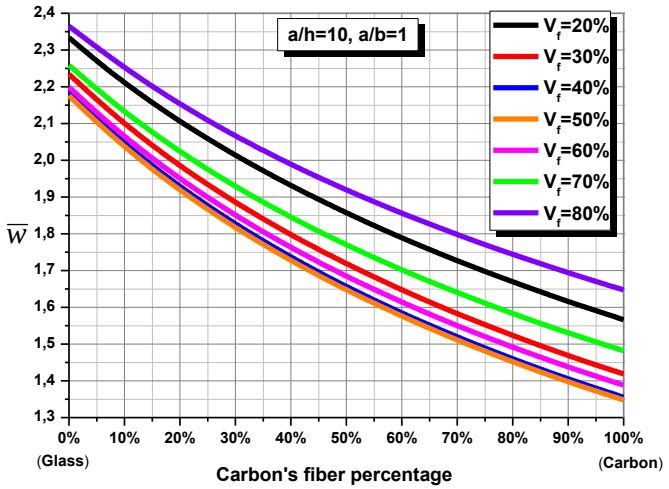

Fig. 2 Dimensionless deflection $\bar{w}$ of a simply supported two-layer (0/90) Carbon /glass-epoxy hybrid square laminates for different values of the fiber's volume fraction V_f

Table 3 and Fig. 2 show the variation of dimensionless deflection of a two-layer cross-ply (0°/90°) square intralayer hybrid composite plates for different values of fiber's volume fraction V_f. It is clearly observed from these data that the displacement is dependent on the variation of the fiber's volume fraction V_f, where the deflection is minimal at V_f=0.5 and it decreases for the other values, which can easily explained by: for V_f values lower than 0.5 the quantity of matrix become much more important compared to the fibers leading to a lower mechanical properties and consequently effect the mechanical behavior of hybrid composite plate in bending. On the other hand, for higher values of V_f the plates become made of almost entirely from fibers (very small quantity of matrix) which means that the plate becomes very fragile, also the matrix in this case can no longer play its role in ensuring the fibers orientation and alignment.

Table 4 The effect of fibers combinations on the variation of dimensionless deflection $\bar{w}$ of a square two layers cross-ply (0/90) Carbon /glass-epoxy hybrid laminates, $V_f = 0.6$

Carbon's fibers percentage w_f (%)		a/h					
Carbon	Glass	2	5	10	20	50	100
0%	100%	5.6952	2.6468	2.1994	2.0870	2.0555	2.0510
10%	90%	5.5205	2.5087	2.0647	1.9532	1.9219	1.9175
20%	80%	5.3577	2.3893	1.9500	1.8396	1.8086	1.8042
30%	70%	5.2112	2.2853	1.8506	1.7412	1.7106	1.7062
40%	60%	5.0792	2.1932	1.7629	1.6546	1.6242	1.6199
50%	50%	4.9597	2.1110	1.6846	1.5773	1.5471	1.5428
60%	40%	4.8508	2.0367	1.6141	1.5076	1.4777	1.4734
70%	30%	4.7510	1.9693	1.5501	1.4443	1.4147	1.4104
80%	20%	4.6591	1.9076	1.4916	1.3866	1.3571	1.3529
90%	10%	4.5740	1.8510	1.4379	1.3336	1.3043	1.3001
100%	0%	4.4950	1.7988	1.3883	1.2847	1.2556	1.2514

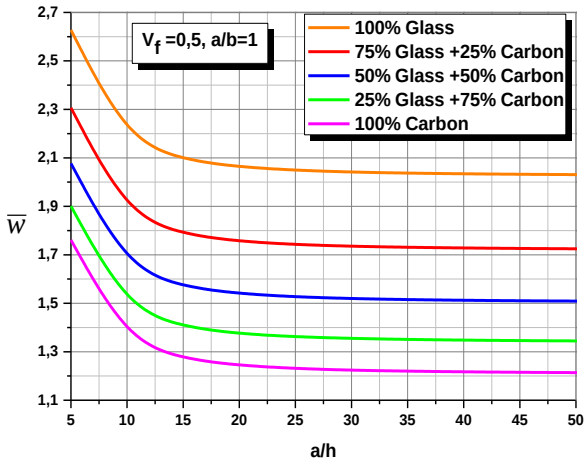

Fig. 3 Variation of dimensionless deflection $\bar{w}$ of a square two-layer (0/90) Carbon /glass-epoxy intralayer hybrid composite plates for various fibers combinations

Table 4 and Fig. 3 illustrate the variation of dimensionless deflection of square cross-ply (0°/90°) intralayer hybrid composite plates for various fiber combinations. Based on the previously illustrated findings, we notice that the deflection is maximal in the case of a Glass-epoxy composite plate, minimal in the case of Carbon-epoxy composite, and varies between these two values for the other Glass/Carbon-epoxy hybrid fiber combinations according to the percentage of carbon fibers introduced in the hybrid plate. Moreover, the combination of two types of fibers in the same layer allows engineers to vary material properties gradually according to their needs. Thanks to this variation, they can control precisely the mechanical behavior of hybrid composite plates, eliminating major defects encountered in conventional composites like delamination, for instance. One other feature of intralayer hybrid composites that needs to be addressed is that the weaknesses of each fiber are compensated for via the employment of other adequate fibers.

Table 5 Effect of stacking sequence on dimensionless deflection $\bar{w}$ of a laminated cross-ply $(0°/90°)_n$ Carbon /glass-epoxy hybrid plate

Number of plies	*a/h*	$\bar{w}$				
		$w_f = 0\%$ (100% Glass)	$w_f = 25\%$ (25% Carbon+75% Glass)	$w_f = 50\%$ (50% Carbon+50% Glass)	$w_f = 75\%$ (75% Carbon+25% Glass)	$w_f = 100\%$ (100% Carbon)
$(0/90)_2$	5	2.1926	1.7415	1.4907	1.3317	1.2217
	10	1.7308	1.2761	1.0248	0.8657	0.7558
	20	1.6151	1.1595	0.9079	0.7487	0.6389
	100	1.5781	1.1222	0.8705	0.7113	0.6014
$(0/90)_3$	5	2.1296	1.6721	1.4258	1.2726	1.1682
	10	1.6685	1.2079	0.9613	0.8083	0.7041
	20	1.5530	1.0916	0.8448	0.6918	0.5875
	100	1.5160	1.0543	0.8075	0.6544	0.5502
$(0/90)_4$	5	2.1078	1.6484	1.4036	1.2523	1.1496
	10	1.6476	1.1856	0.9408	0.7898	0.6875
	20	1.5323	1.0696	0.8247	0.6738	0.5715
	100	1.4955	1.0325	0.7876	0.6366	0.5343
$(0/90)_5$	5	2.0978	1.6375	1.3934	1.2429	1.1409
	10	1.6381	1.1755	0.9316	0.7816	0.6801
	20	1.5230	1.0597	0.8158	0.6658	0.5643
	100	1.4861	1.0227	0.7787	0.6287	0.5272
$(0/90)_6$	5	2.0923	1.6316	1.3878	1.2378	1.1362
	10	1.6329	1.1701	0.9266	0.7771	0.6761
	20	1.5179	1.0545	0.8110	0.6615	0.5605
	100	1.4811	1.0174	0.7739	0.6245	0.5235
$(0/90)_8$	5	2.0869	1.6257	1.3823	1.2327	1.1315
	10	1.6279	1.1648	0.9217	0.7728	0.6721
	20	1.5129	1.0492	0.8062	0.6573	0.5568
	100	1.4761	1.0123	0.7693	0.6204	0.5198
$(0/90)_{16}$	5	2.0817	1.6200	1.3769	1.2278	1.1270
	10	1.6230	1.1596	0.9171	0.7686	0.6684
	20	1.5081	1.0443	0.8017	0.6533	0.5532
	100	1.4714	1.0073	0.7648	0.6164	0.5163

Tables 5 and 6 represent the variation of dimensionless deflection of laminated cross-ply $(0°/90°)_n$ and angle-ply $(45°/-45°)_n$ intralayer hybrid composite plates for various fiber combinations, stacking sequences and side-to-thickness ratios. In every single case Carbon/Glass fiber combination, this dimensionless deflection decreases with the increase of the stacking sequence (number of plies) and the side to thickness ratio *a/h*, which is logical for the reason that the thickness ratio means that a condensation of fibers in a thin plate is occurring. It is concluded that for stiffness and economic whys and wherefores, the recommended stacking sequence is eight plies ($(45°/-45°)_4$ and $(0°/90°)_4$).

Table 6 Effect of stacking sequence on dimensionless deflection $\bar{w}$ of a laminated angle-ply $(45°/-45°)_n$ Carbon /glass-epoxy hybrid plate

Number of plies	*a/h*	$\overline{w}$				
		$w_f = 0\%$ (100% Glass)	$w_f = 25\%$ (25% Carbon +75% Glass)	$w_f = 50\%$ (50% Carbon +50% Glass)	$w_f = 75\%$ (75% Carbon +25% Glass)	$w_f = 100\%$ (100% Carbon)
$(45/-45)_2$	5	1.7017	1.3170	1.1340	1.0269	0.9564
	10	1.2395	0.8516	0.6685	0.5619	0.4920
	20	1.1237	0.7349	0.5516	0.4449	0.3750
	100	1.0866	0.6975	0.5141	0.4074	0.3375
$(45/-45)_3$	5	1.6472	1.2662	1.0902	0.9889	0.9229
	10	1.1859	0.8022	0.6263	0.5256	0.4604
	20	1.0703	0.6858	0.5098	0.4091	0.3439
	100	1.0333	0.6485	0.4725	0.3718	0.3065
$(45/-45)_4$	5	1.6283	1.2485	1.0746	0.9750	0.9104
	10	1.1681	0.7861	0.6127	0.5139	0.4501
	20	1.0528	0.6701	0.4967	0.3979	0.3342
	100	1.0159	0.6330	0.4595	0.3607	0.2970
$(45/-45)_5$	5	1.6196	1.2402	1.0673	0.9685	0.9044
	10	1.1601	0.7789	0.6066	0.5086	0.4455
	20	1.0449	0.6631	0.4908	0.3929	0.3299
	100	1.0080	0.6260	0.4537	0.3558	0.2928
$(45/-45)_6$	5	1.6148	1.2357	1.0633	0.9649	0.9011
	10	1.1557	0.7750	0.6033	0.5058	0.4430
	20	1.0406	0.6594	0.4877	0.3903	0.3276
	100	1.0038	0.6223	0.4506	0.3532	0.2906
$(45/-45)_8$	5	1.6101	1.2313	1.0593	0.9612	0.8978
	10	1.1514	0.7711	0.6000	0.5030	0.4406
	20	1.0364	0.6557	0.4846	0.3877	0.3253
	100	0.9996	0.6187	0.4476	0.3507	0.2884
$(45/-45)_{16}$	5	1.6055	1.2269	1.0554	0.9577	0.8945
	10	1.1473	0.7675	0.5969	0.5003	0.4382
	20	1.0324	0.6521	0.4816	0.3852	0.3232
	100	0.9957	0.6152	0.4447	0.3483	0.2863

The effect of fiber's orientation on the variation of dimensionless deflection of laminated hybrid composite plates is illustrated on Table 7 and Fig. 4 for different fiber combinations and aspect ratio (*a/b*), from which this deflection varies according to the fiber's orientation angle. Although, deflection is not the sole criterion to consider when opting for an orientation angle; several parameters, including the geometry of the plate, must also be considered for optimal results.

As demonstrated in Figs. 5-8 the plane of normal stresses, $\bar{\sigma}_{xx}$ and $\bar{\sigma}_{yy}$ are distributed throughout the plate thickness in compression until the plate's middle-Hight (*z*=0), at which point they turn into tension. Whereas, based on Figs. 9 and 10 we notice that a position on the plate's top

Table 7 Effect of fiber orientation and aspect ratio *a/b* on the dimensionless deflection $\bar{w}$ of a laminated Carbon /glass-epoxy hybrid plate

Fiber's orientation	*a/b*	$\overline{w}$				
		$w_f = 0\%$ (100% Glass)	$w_f = 25\%$ (25% Carbon +75% Glass)	$w_f = 50\%$ (50% Carbon +50% Glass)	$w_f = 75\%$ (75% Carbon +25% Glass)	$w_f = 100\%$ (100% Carbon)
$(0/90)_4$	1	1.6476	1.1856	0.9408	0.7898	0.6875
	2	0.2657	0.1962	0.1618	0.1414	0.1279
	3	0.0766	0.0602	0.0524	0.0478	0.0448
$(15/-15)_4$	1	1.4770	1.0334	0.8122	0.6802	0.5924
	2	0.4073	0.3383	0.2919	0.2589	0.2343
	3	0.1333	0.1212	0.1115	0.1036	0.0972
$(30/-30)_4$	1	1.2551	0.8527	0.6652	0.5570	0.4866
	2	0.3077	0.2328	0.1928	0.1680	0.1512
	3	0.1051	0.0864	0.0752	0.0677	0.0625
$(45/-45)_4$	1	1.1681	0.7861	0.6127	0.5139	0.4501
	2	0.2450	0.1792	0.1480	0.1299	0.1180
	3	0.0818	0.0644	0.0558	0.0507	0.0473

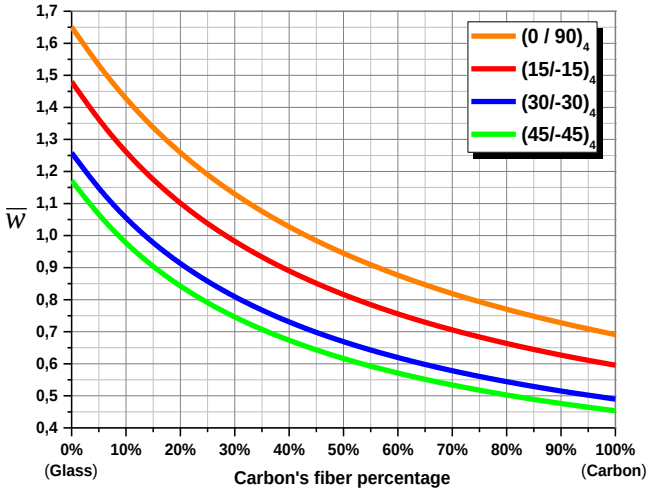

Fig. 4 Effect of fiber orientation and combination on the dimensionless deflection $\bar{w}$ of a square laminated Carbon /glass-epoxy hybrid plate

and bottom surfaces, respectively, is where the shear stress's $\bar{\tau}_{xy}$ tensile and compressive strength readings are the highest. Furthermore, the breaks noted in the illustrated curves are a result of the abrupt change in the plate's interlaminar stiffness.

5. Conclusions

A simple and precise refined high order shear deformation theory was used successfully to

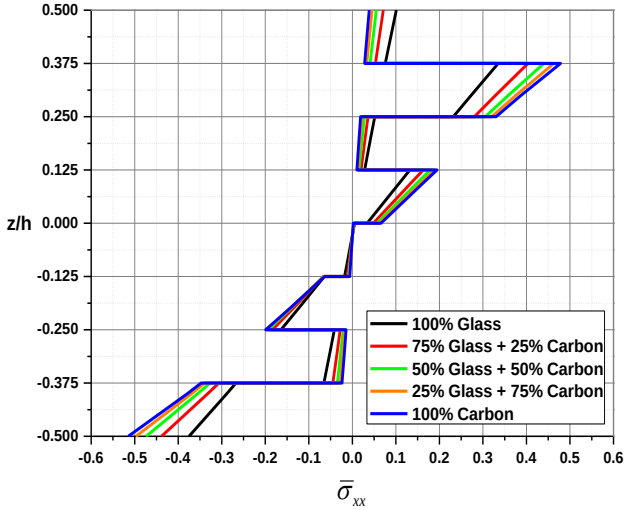

Fig. 5 Variation of dimensionless normal stress $\bar{\sigma}_{xx}$ across the thickness of a square laminated cross-ply $(0°/90°)_4$ Carbon /glass-epoxy hybrid plate

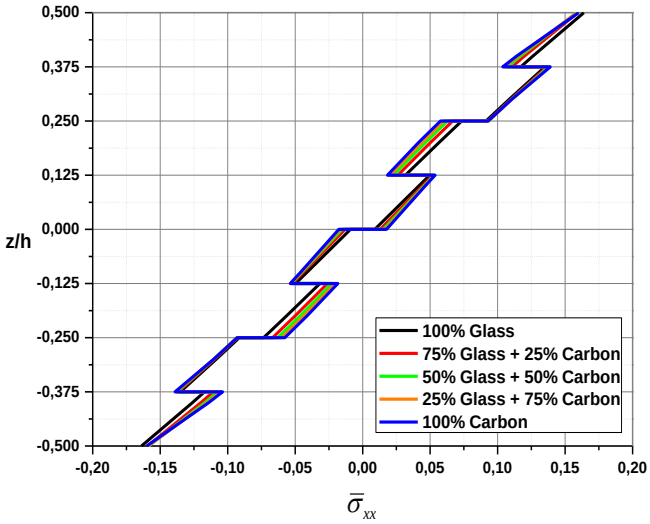

Fig. 6 Variation of dimensionless normal stress $\bar{\sigma}_{xx}$ across the thickness of a square laminated angle-ply $(45°/-45°)_4$ Carbon /glass-epoxy hybrid plate

study the bending behavior of a carbon/glass-epoxy hybrid laminated composite plates. The present theory's efficiency and precision have been undoubtedly demonstrated by comparing the obtained results with those issued from the literature for the case of bending behavior of carbon/glass-epoxy hybrid composite plates.

Based on the present study, we obtain the following conclusions:

• The present refined high-order theory is reliable, precise and time-effective in analyzing the mechanical behavior of hybrid composite plates.

• The deformations and stresses are dependent on various parameters like plate's geometry,

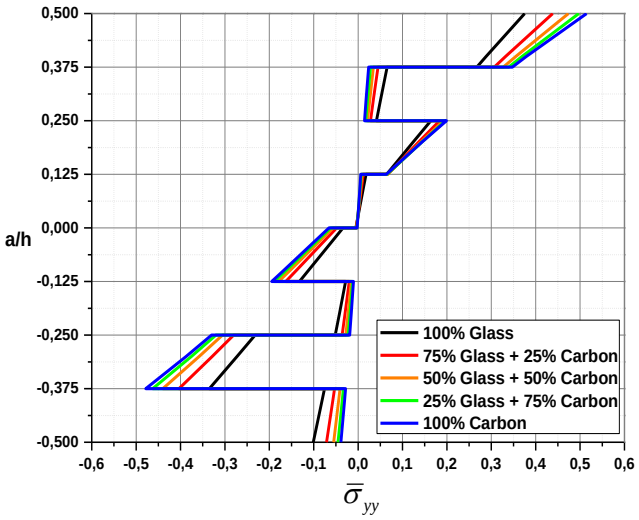

Fig. 7 Variation of dimensionless normal stress $\bar{\sigma}_{yy}$ across the thickness of a square laminated cross-ply $(0°/90°)_4$ Carbon/glass-epoxy hybrid plate

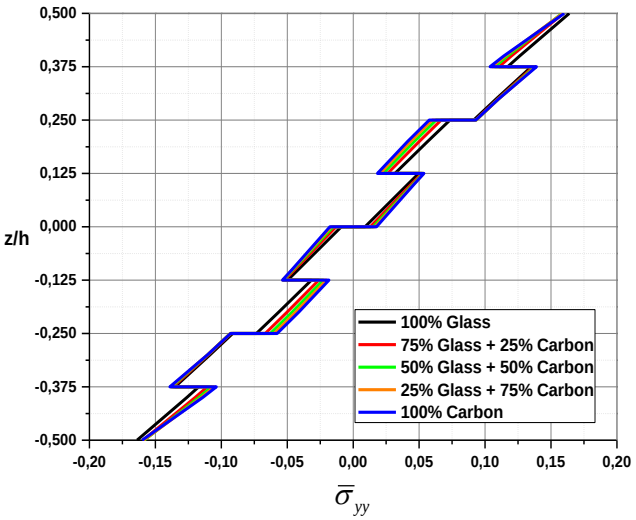

Fig. 8 Variation of dimensionless normal stress $\bar{\sigma}_{yy}$ across the thickness of a square laminated angle-ply $(45°/-45°)_4$ Carbon/glass-epoxy hybrid plate

fibers orientation and stacking effect.

• The material properties in hybrid composites plays a crucial role in the plate's overall behavior, where the choice of the types of fibers and their volume fractions is vital for hybrid composites.

To sum up, the key reason for adopting glass and carbon fibers in this research is that, while carbon fibers guarantee a higher mechanical characteristic, this strength is limited by their costly price tag. On the other hand, glass fibers are cheaper in addition to exhibiting a poor mechanical property. Therefore, to get the most of this hybrid composites, we are encouraged to search for the

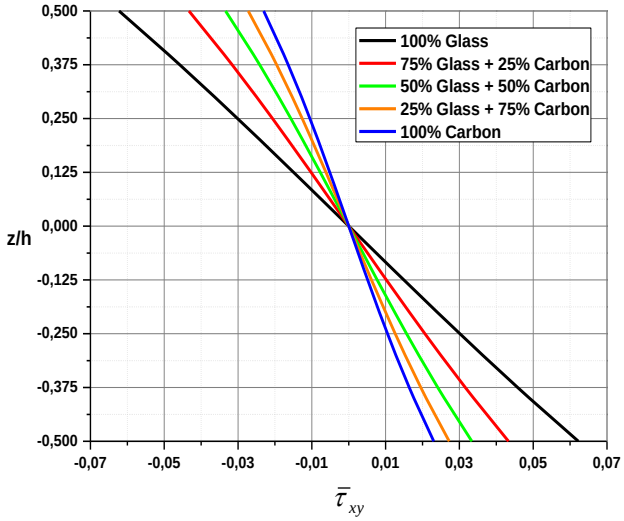

Fig. 9 Variation of dimensionless shear stress $\bar{\tau}_{xy}$ across the thickness of a square laminated cross-ply $(0°/90°)_4$ Carbon /glass-epoxy hybrid plate

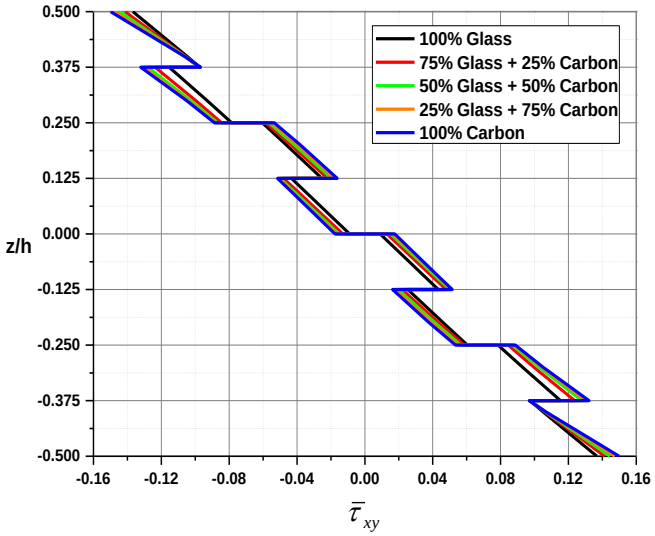

Fig. 10 Variation of dimensionless shear stress $\bar{\tau}_{xy}$ across the thickness of a square laminated angle-ply $(45°/-45°)_4$ Carbon /glass-epoxy hybrid plate

adequate combination between these two types of fibers to benefit from their features and consequently eliminate their limitations.

References

Adim, B. and Daouadji, T.H. (2024), "Analysis of the hygro-thermo-mechanical response of functionally

graded plates resting on elastic foundations based on various micromechanical models", *Geomech. Eng.*, **38**(4), 409-420. https://doi.org/10.12989/gae.2024.38.4.409.

Adim, B., Daouadji, T.H., Rabia, B. and Hadji, L. (2016), "An efficient and simple higher order shear deformation theory for bending analysis of composite plates under various boundary conditions", *Earthq. Struct.*, **11**(1), 63-82. https://doi.org/10.12989/eas.2016.11.1.063.

Alarifi, I.M. and Asmatulu, R. (2023), "12-Hybrid nanocomposite materials", *Advanced Hybrid Composite Materials and their Applications*, 237-255.

Berthelot, J.M. (2005), *Matériaux Composites: Comportement Mécanique Et Analyse des Structures*, 5th Edition, Editions Tec & Doc Lavoisier, Paris, France.

Berthelot, J.M. (2010), *Mécanique des Matériaux et Structures Composites*, Institut Supérieur des Matériaux et Mécaniques Avancés, Le Mans, France.

Daouadji, T.H., Benferhat, R. and Adim, B. (2016a), "Bending analysis of an imperfect advanced composite plates resting on the elastic foundations", *Couple. Syst. Mech.*, **5**(3), 269-283. https://doi.org/10.12989/csm.2016.5.3.269.

Daouadji, T.H., Benferhat, R. and Adim, B. (2016b), "A novel higher order shear deformation theory based on the neutral surface concept of FGM plate under transverse load", *Adv. Mater. Res.*, **5**(2), 107-120. http://doi.org/10.12989/amr.2016.5.2.107.

Daouadji, T.H., Chedad, A. and Adim, B. (2016c), "Interfacial stresses in RC beam bonded with a functionally graded material plate", *Struct. Eng. Mech.*, **60**(4), 693-705. https://doi.org/10.12989/sem.2016.60.4.693.

De Matos, G.B.A. and Júnior, E.P. (2024), "Isogeometric analysis of functionally graded plates using high-order theories", *Ibero-Latin American Congress on Computational Methods in Engineering (CILAMCE)*, Maceió, Brazil, November.

Dewangan, H.C. and Panda, S.K. (2021), "Numerical transient responses of cut-out borne composite panel and experimental validity", *Proc. Inst. Mech. Eng., Part G: J. Aerosp. Eng.*, **235**(11), 1521-1536. https://doi.org/10.1177/0954410020977344.

Drobnjak, I. (2023), "The role of fiber-reinforced polymer composites in civil engineering", *J. Facult. Civil Eng. Arch.*, **38**, 52-63. https://doi.org/10.62683/ZRGAF38.52-63.

Furtmüller, T. and Adam, C. (2022), "A higher-order plate theory for the analysis of vibrations of thick orthotropic laminates", *Acta Mechanica*, **233**(10), 3941-3956. https://doi.org/10.1007/s00707-022-03302-7.

Georgantzinos, S.K., Giannopoulos, G.I., Stamoulis, K. and Markolefas, S. (2023), "Composites in aerospace and mechanical engineering", *Mater.*, **16**(22), 7230. https://doi.org/10.3390/ma16227230.

Henni, M.A.B., Abbès, B., Daouadji, T.H., Abbès, F. and Adim, B. (2021), "Numerical modeling of hygrothermal effect on the dynamic behavior of hybrid composite plates", *Steel Compos. Struct.*, **39**(6), 751-763. https://doi.org/10.12989/scs.2021.39.6.751.

Jain, N. and Kathuria, S. (2024), *Utilizing Friction Stir Techniques for Composite Hybridization*, IGI Global, Pennsylvania, USA.

Kant, T.A.R.U.N. and Swaminathan, K. (2002), "Analytical solutions for the static analysis of laminated composite and sandwich plates based on a higher order refined theory", *Compos. Struct.*, **56**(4), 329-344. https://doi.org/10.1016/S0263-8223(02)00017-X.

Keller, T. (2024), *Composites in Structural Engineering and Architecture*, EPFL Press, Lausanne, Switzerland.

Kırad, A., Muthanna, B.G.N., Madanı, F. and Zeddam, L. (2023), "Numerical study of the mechanical behavior of a composite material plate", *Eurasia Proc. Sci. Technol. Eng. Math.*, **26**, 458-461. https://doi.org/10.55549/epstem.1411062.

Kulkarni, M.V. and Boppana, S.B. (2023), *Composites Overview, Structural Composite Materials: Fabrication, Properties, Applications and Challenges*, Springer Nature, Singapore, Singapore.

Kumar, V., Dewangan, H.C., Sharma, N., Panda, S.K. and Mahmoud, S.R. (2023), "Nonlinear deflection characteristics of damaged composite structure theoretical prediction and experimental verification", *Struct.*, **52**, 410-421. https://doi.org/10.1016/j.istruc.2023.03.147.

Latheswary, S., Valsarajan, K.V. and Rao, Y.S. (2003), "Behaviour of shear deformable plate bending finite

elements for composites", *J. Aerosp. Sci. Technol.*, **55**(3), 223-230. https://doi.org/10.61653/joast.v55i3.2003.762.

Monteiro, B. and Simões, S. (2024), "Recent advances in hybrid nanocomposites for aerospace applications", *Metal.*, **14**(11), 1283. https://doi.org/10.3390/met14111283.

Nadaf, M. and Fernandes, R.J. (2023), "Bending analysis for stress and deflection for cross-ply laminated composite plate using higher order shear deformation theory subjected to sinusoidal loading using finite element method", *Indian J. Sci. Technol.*, **16**(38), 3177-3185. https://doi.org/10.17485/IJST/v16i38.1435.

Pagano, N.J. (1970), "Exact solutions for rectangular bidirectional composites and sandwich plates", *J. Compos. Mater.*, **4**(1), 20-34. https://doi.org/10.1177/002199837000400102.

Pandey, H.K., Agrawal, H., Panda, S.K., Hirwani, C.K., Katariya, P.V. and Dewangan, H.C. (2020), "Experimental and numerical bending deflection of cenosphere filled hybrid (Glass/Cenosphere/Epoxy) composite", *Struct. Eng. Mech.*, **73**(6), 715-724. https://doi.org/10.12989/sem.2020.73.6.715.

Pandya, B.N. and Kant, T. (1988), "Finite element analysis of laminated composite plates using a higher-order displacement model", *Compos. Sci. Technol.*, **32**(2), 137-155. https://doi.org/10.1016/0266-3538(88)90003-6.

Rabahi, A., Adim, B., Chargui, S. and Daouadji, T.H. (2014), "Interfacial stresses in FRP-plated RC beams: effect of adherend shear deformations", *Conference on Multiphysics Modelling and Simulation for Systems Design*, Springer International Publishing, Hammamet, December.

Ramu, T., Naik, P. and Reddy, B.S. (2024), "Hybrid composite materials from crotalaria and borassus fibers: Mechanical and water absorption properties", *J. Solid Waste Technol. Manage.*, **50**(5), 775-786. https://doi.org/10.5276/jswtm/iswmaw/504/2024.775.

Sahu, P., Sharma, N., Dewangan, H.C. and Panda, S.K. (2022a), "Theoretical prediction and experimental validity of thermal frequency responses of laminated advanced fiber-reinforced epoxy hybrid composite panel", *Int. J. Struct. Stab. Dyn.*, **22**(08), 2250088. https://doi.org/10.1142/S0219455422500882.

Sahu, P., Sharma, N., Dewangan, H.C. and Panda, S.K. (2022b), "Thermo-mechanical transient flexure of glass-carbon-kevlar-reinforced hybrid curved composite shell panels: An experimental verification", *Int. J. Appl. Mech.*, **14**(01), 2150120. https://doi.org/10.1142/S1758825121501209.

Sundeep, M. and Baddepudi, M. (2023), "Analytical study on bending behaviour of plates made of functionally graded materials using higher-order shear", *Mater. Today: Proc.*, https://doi.org/10.1016/j.matpr.2023.06.239.

Thai, H.T. and Kim, S.E. (2013), "A simple higher-order shear deformation theory for bending and free vibration analysis of functionally graded plates", *Compos. Struct.*, **96**, 165-173. https://doi.org/10.1016/j.compstruct.2012.08.025.

Vasiliev, V.V. and Morozov, E.V. (2001), *Mechanics and Analysis of Composite Materials*, 1st Edition, Elsevier, New York, USA.

Xiang, S. and Kang, G.W. (2013), "A *n*th-order shear deformation theory for the bending analysis on the functionally graded plates", *Eur. J. Mech.-A/Solid.*, **37**, 336-343. https://doi.org/10.1016/j.euromechsol.2012.08.005.

Zozulya, V.V. (2018a), "Higher order theory of micropolar plates and shells", *ZAMM-J. Appl. Math. Mech.*, **98**(6), 886-918. https://doi.org/10.1002/zamm.201700317.

Zozulya, V.V. (2018b), "Higher order couple stress theory of plates and shells", *ZAMM-J. Appl. Math. Mech.*, **98**(10), 1834-1863. https://doi.org/10.1002/zamm.201800022.